https://doi.org/10.33271/nvngu/2022-3/067

O. O. Tytov[1],
orcid.org/0000-0001-6794-8240,
V. P. Nadutyy[2],
orcid.org/0000-0002-2453-0351,
K. V. Babii[2],
orcid.org/0000-0002-0733-2732,
D. L. Kolosov[1],
orcid.org/0000-0003-0585-5908,
V. Yu. Kukhar[1],
orcid.org/0000-0002-1849-4489

1 – Dnipro University of Technology, Dnipro, Ukraine, e-mail: tytov.o.o@nmu.one
2 – Institute of Geotechnical Mechanics named by N. Poljakov, Dnipro, Ukraine

FLAT PROBLEM TO DETERMINE THE FORCES OF DESTRUCTION OF PIECES IN DISINTEGRATORS WHILE BEING GRABBED IN THICK LAYER

Purpose. Research on analytical dependences of destructive stresses, acting on a piece of non-isometric shape at quasi-static deformation of a relatively thick layer of rock mass in disintegrators, on parameters of the piece shape, the piece's spatial orientation, also on the relative piece size in layer, taking into consideration the discrete nature of contact force application.

Methodology. The flat scheme of a non-isometric shaped piece contacts in a thick layer of rock mass is obtained by composition of the central rectangular piece and the round pieces of average size for the given layer. The distribution of stress components in the layer of loose rock mass is accepted on the basis of the classical theory of elasticity and the theory of loose medium. The geomechanics criterion showing relationship of equivalent destructive stress and ultimate compressive strength of rock is used as a criterion of piece destruction in complex stress state. All force schemes of the piece loading are reduced to three-point bending schemes and two-point shear schemes, both across the long and the short sides of the piece. The most dangerous loading scheme is determined from the analysis of the mentioned schemes for each particular case. Dimensionless parameterization is applied both to specify the geometric parameters of pieces and to analyze the resulting destructive stresses.

Findings. Analytical dependences of equivalent destructive stresses for an oblong piece are obtained depending on the piece relative length, the relative piece size in the rock layer, the angle of piece orientation relative to the direction of the maximum main stress and the side thrust coefficient in the layer. It has been set that lamellar pieces, especially those smaller than the average size for the layer, are destroyed mainly from the implementation of bending schemes across the long side, the shape of their fragments is improved by reducing the pieces' relative length. Increasing the uniformity of the force field in the working zone of disintegrator also leads to improvement in the shape of fragments. On the other hand, as the shape of the piece approaches the isometric one, as well as when the piece relative size in layer raises, the probability of implementing shear schemes increases and the probability of implementing bending schemes decreases, including with a deterioration in the fragments shape compared to the original piece. At the same time, larger values of destructive stresses for the lamellar smaller pieces are proved analytically compared to the isometric bigger ones, all other things being equal.

Originality. The versatility of application of the three-point bending scheme of a non-isometric shaped piece in combination with the two-point scheme of its shear for analysis of its destruction in the thick layer of rock mass is substantiated. For the first time, the dependences of equivalent destructive stresses for the non-isometric piece on its relative length, its relative size in layer, the angle of deviation of the piece's main axis from the main stress direction and on the side thrust coefficient in the layer have been obtained.

Practical value. The results obtained allow making reasonable choice of parameters of disintegrators' operational parts for destruction of materials in the thick layer, as well as predicting the change in lamellar pieces fraction during disintegration process. They give the possibility to determine key parameters of operational parts for new designs of disintegrators. This creates the basis for the development of calculation techniques for operational parts of modern samples of crushing and grinding equipment.

Keywords: *disintegrator, thick layer, complex stress state, lamellar piece, bend, shear, side thrust coefficient*

Introduction. Disintegrators of various designs are used for processing rock mass and technogenic rock raw materials [1].

Analysis of destruction features for pieces of rocks in operation area is of particular interest when determining rational parameters of operational parts of disintegrators. Usually, it is necessary to establish a way for applying a load to material from operational parts of a disintegrator for a given source material, determine a sufficient level of destructive forces, and, based on this, design an operational part.

In a broader sense, it is necessary to justify a promising design of a disintegrator by synthesizing a force field of such a configuration, which is best suited for processing a given material.

Therefore, various models of rock pieces and models of their loading are used for this.

Models of a single piece deformation between two rigid operational surfaces are very common, which are relevant for some types of crushers, for example, jaw crushers [2]. A compression of an isometric piece is considered here when two plates located at an angle to each other approach each other. The purpose of this is subsequent determination of a limiting destructive force for a given piece size.

However, there are many other configurations of capturing and destroying the pieces, especially deformation of pieces of a non-isometric shape, destruction by shear and bending, destruction due to forces of inertia upon impact with a rigid barrier, as well as the so-called "destruction in the layer". In the latter case, it is about a deformation of a relatively thick layer of rock mass, when a piece size is noticeably smaller than a layer thickness (hereinafter simply "thick layer"). Considering these configurations makes it possible to simulate the physics of a process of mass destruction of pieces more accurately and is especially relevant for calculation models of new units of crushing and grinding equipment.

In particular, destruction in a thick layer is typical for disintegrators operating with fine-grained and fine-dispersed material, when it is impossible or undesirable to clamp material with a thickness of one particle between the operational surfaces. The literature describes the effects of a decrease in lamellar particles in the output observed in this case and selective destruction along the grain boundaries of various minerals [3]. However, there is a scientific problem of establishing a dependence between the influence of layer parameters and force field parameters on characteristics of the obtained products, which will allow effective control of the process.

Literature review. It is known that the quality of crushed stone increases with a decrease in lamellar particle yield in the output, in accordance with the standard DSTU B V.2.7-75-98. In this regard, the disintegrators, which ensure the primary destruction of specifically lamellar particles compared to isometric ones, are more suitable for crushed stone production. It is known that cone crushers with a special design of a crushing chamber, in which loads are implemented in a multilayer mass of pieces, for example, "Girodisk" [2], provide a lower output of lamellar particles than traditional cone crushers, have an increased degree of crushing and a reduced specific energy intensity of the process. The explanation for this positive effect is that when crushed in a thick layer, one piece is in contact with several pieces surrounding it, instead of two operational surfaces when crushing in one layer using traditional crushers, and a multiplicity of options for destruction planes to pass through a piece ensures, at least, a better destruction of lamellar particles.

It should be noted, that these effects are only described qualitatively, without a detailed study on a mechanism of influence of a stress state in a thick layer on destruction of a piece of a given (non-isometric) shape.

In this regard, there is a need for further study on the following aspects of the problem:

1) distribution of stresses in a layer of loose material;

2) criteria for destruction of pieces in a three-dimensional stressed state;

3) justification of the most dangerous type of load for pieces (compression, shear, bending) for random piece orientation relatively to an operational part of a disintegrator;

4) consideration of a discrete character of loading the pieces at several points in comparison with a continuous medium model;

5) justification of a comparative level of destructive loads for pieces of different sizes (selection function).

Movement of crushing elements of machines with quasi-static action can almost always be reduced to compression of a layer, optionally combined with application of transverse shear forces. Presence of a shear increases the destruction efficiency of pieces and reduces the energy consumption for crushing [3].

Configuration of a force field inside the operation zone of disintegrators, limited by their operating surfaces, has a non-uniform character and, under a purely compressive load, can be determined in accordance with [4] by the following expression

$$\sigma_3 = \xi(\varepsilon_0, \sigma_1)\sigma_1, \tag{1}$$

where σ_1 is maximum main stress acting along the direction of compression; σ_3 is minimum main stress acting in the transverse direction; ε_0 is the initial coefficient of layer porosity; $\xi(\varepsilon_0, \sigma_1)$ is side thrust coefficient.

The side thrust coefficient in loose material depends on the coefficient of internal friction, which, in turn, depends on a presence of moisture in the material [5], but consideration of these issues is not the subject of this article.

In the presence of a shear load, external shear stresses additionally act on opposite operating surfaces, usually equal in magnitude and opposite in direction. In this case, components of a stress state can also be reduced to the values σ_1 and σ_3 in accordance with the laws of elasticity theory, for example [6] or [7]. Here equality (1) will be fulfilled, but the direction of σ_1 will no longer coincide with the direction of compression.

The paper [8] is of particular interest in terms of a fracture criterion in relation to real rocks. This paper gives a relation of equivalent destructive stress with parameters of complex stress state and compressive strength of the material

$$\sigma_e = \frac{(\psi-1)(\sigma_1+\sigma_3)}{2\psi} + \frac{\sqrt{(1-\psi)^2(\sigma_1+\sigma_3)^2+4\psi(\sigma_1-\sigma_3)^2}}{2\psi} \geq R_c, \tag{2}$$

where R_c is material compressive strength; ψ is the plasticity coefficient.

This criterion is deduced in conformity to a small element of rock mass, located inside a fairly large massif. Based on this criterion, an analysis, for example, of a crack initiation in a rock mass is performed [9].

In a case when a space is filled with individual rock pieces, even if they are densely packed, a stressed state of a piece can no longer obey the laws of continuum mechanics. So, some average piece of rock mass is characterized by a coordination number, which is equal to the number of pieces that are in contact with it. The densest packing can only be obtained by filling a space with pieces of different sizes with a definite ratio of their number, while a coordination number is large enough and a load on a surface of a particular piece approaches the load that is applied to an element of a continuous medium. However, in reality, a number of contacts is small due to a rather large layer porosity, so each contact acts as a stress concentrator, which makes it necessary to consider the discreteness of load application to pieces.

In addition to the latter circumstance, the pieces also differ significantly in size, so a stress level depends on a ratio of sizes of the considered piece and pieces around it. The action of this factor is called the "selection function" in the literature [10].

Unsolved aspects of the problem. Thus, it is necessary to find a response to issues regarding the model representation of geometry of a calculated piece, the distribution of stresses in a layer, the model representations of application of a discrete load to a piece, the determination of destructive stresses considering the selected fracture criterion, the size and shape of a piece, the piece orientation relatively to directions of main stresses, as well as the comparative probability of destruction of a given piece in the thick layer of rock mass.

Main part. ***Scheme justification for piece bending in a thick layer.*** In paper [11], the problems of bending with longitudinal compression of elongated pieces in different types of force fields, typical for roller and centrifugal disintegrators, are considered. It is shown that bending deformations lead to occurrence of destructive stresses several times greater than the stresses during simple compression of a piece between two operational surfaces. Dependences of equivalent destructive stresses on a relative piece length are established

$$k_{ca} = \frac{c}{a},$$

where the minimum, average and maximum dimensions of a piece with corresponding values *a*, *b* and *c* are previously designated.

Thus, for a case of deformation of a piece in the thick layer, it is necessary to establish a mechanism for implementing a force scheme associated with bending.

First, let us introduce basic assumptions for flat calculation schemes:

1) a deformable piece of rock mass has a rectangular shape, determined by the thickness *a* and length *c*;

2) a piece is in contact only with pieces of average size for a given layer, having shape of a circle of D_{av} diameter;

3) average-sized pieces are densely packed around the central piece.

Selection of shapes of pieces must be described separately.

A considered rectangular piece shape, on the one hand, makes it possible to take into account its real elongated shape, and, on the other hand, is quite simple and convenient for analysis. Shape complication does not make much sense due to the diversity of a real geometry of pieces. A transition from the model to the real piece shape is performed using the filling coefficient [11]

$$k_f = \frac{V}{a \cdot b \cdot c},$$

where V is particle volume.

A round shape of an average-sized piece is chosen due to the uniformity of a generatrix radius vector in all directions and the absence of a need to consider the orientation of the longitudinal axis of each average-sized piece in space, in order to simplify the analysis.

In general, a composition of a rectangular piece surrounded by several round pieces simulates a satisfactory model of relative position of pieces in a layer, whose main parameter, from the point of view of the bending force scheme, is a distance between adjacent contacts of a considered piece. We will compare the latter value with the piece dimensions.

Consider a three-point piece bending on the long side (Fig. 1, *a*) for the case of layer compression along the *x*-axis,

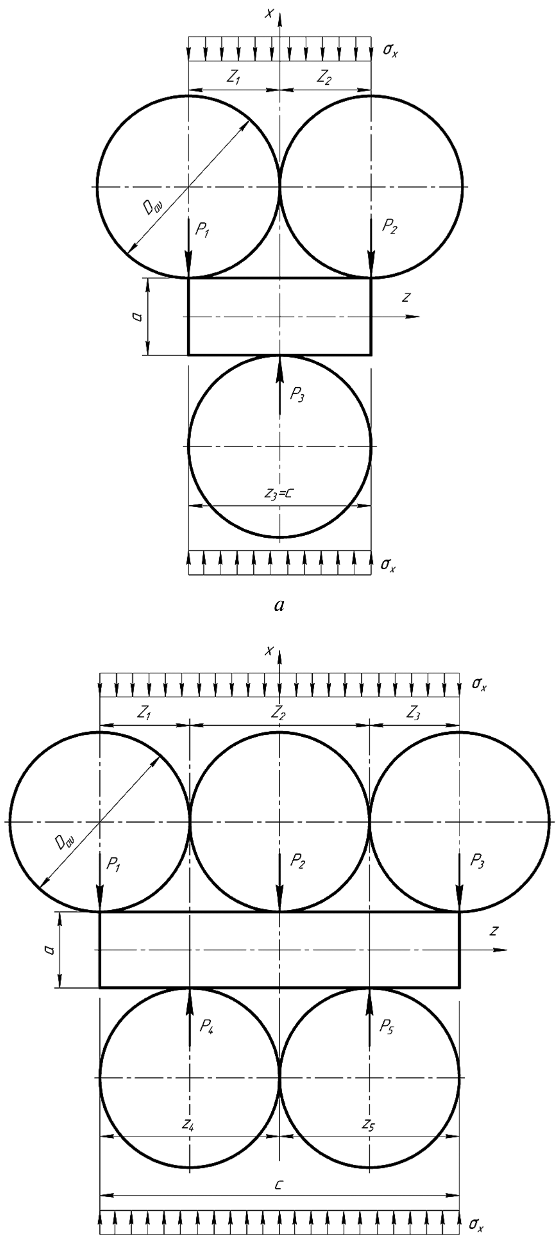

Fig. 1. Schemes of piece bending:
a – three-point; b – five-point

corresponding to the relative piece size in a layer $\lambda = 1$, which is determined by the expression

$$\lambda = \frac{c}{D_{av}}.$$

Here, three middle pieces are involved in a deformation of the central piece, having loading areas with the corresponding lengths z_1, z_2 and z_3

$$z_1 = z_2 = \frac{D_{av}}{2};$$

$$z_3 = D_{av},$$

on which contact forces depend

$$P_1 = P_2 = \frac{\sigma_x b D_{av}}{2n};$$

$$P_3 = \frac{\sigma_x b D_{av}}{n},$$

where b is width along y-axis, which is equal for all pieces; n is layer porosity of the deformed rock mass.

The maximum bending moment in this scheme is observed in the cross-section of a piece along *xy*-plane and is equal to

$$M_{f,\max} = \frac{P_3 D_{av}}{4} = \frac{\sigma_x b D_{av}{}^2}{4n}. \quad (3)$$

It should be noted, that the scheme shown in Fig. 1, *a*, corresponds to the maximum possible bending moment under the given conditions. If the contacts at the piece bottom are displaced by an amount $(c/2)$, so that there are two contacts at the bottom, we obtain a completely symmetrical scheme with zero bending moment. Thus, the whole variety of cases of bending can be simplified to the case with a bending moment $M_{f,\max}$ and to the case with zero bending moment, implemented with a probability of $^1\!/_2$ each.

For a parameter value $\lambda = 2$ we have a five-point bending scheme (Fig. 1, *b*), where the following relations are true

$$z_1 = z_3 = \frac{D_{av}}{2};$$

$$z_2 = z_4 = z_5 = D_{av};$$

$$P_1 = P_3 = \frac{\sigma_x b D_{av}}{2n};$$

$$P_2 = P_4 = P_5 = \frac{\sigma_x b D_{av}}{n};$$

$$M_{f,\max} = \frac{P_4 D_{av}}{4} = \frac{\sigma_x b D_{av}^2}{4n}. \quad (4)$$

It can be concluded from expressions (3, 4) that the maximum bending moment is directly proportional to an axial stress σ_x, to a square of the value D_{av}, and is inversely proportional to a layer porosity n and does not depend on a parameter λ.

A seven-point bending scheme is considered similarly for $\lambda = 3$, nine-point scheme for $\lambda = 4$ etc., with the same conclusions.

The case when $\lambda < 1$, shown in Fig. 2 is of particular interest.

Here, contact forces from the first and second pieces of the size D_{av}, same as in Fig. 1, *a*, are applied at particle corners, but they have additional horizontal components $P_{1,z} = P_{2,z}$, that do not contribute to creation of a bending moment. The lengths of loading areas no longer depend on a value D_{av} and are determined in the following way

$$z_1 = z_2 = \frac{c}{2}; \quad z_3 = c.$$

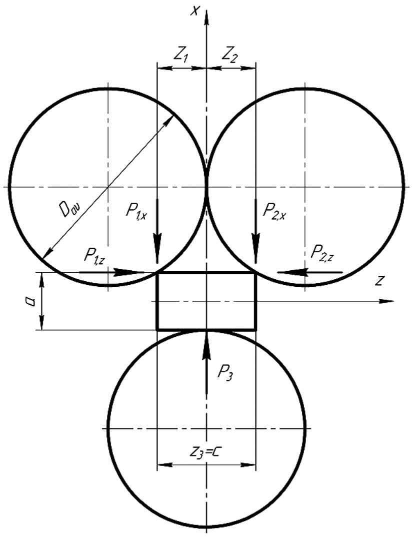

Fig. 2. Three-point scheme of piece bending at $\lambda < 1$

Accordingly, we obtain the following

$$P_{1,x} = P_{2,x} = \frac{\sigma_x bc}{2n}; \quad P_3 = \frac{\sigma_x bc}{n};$$
$$M_{f,\max} = \frac{\sigma_x bc^2}{4n} = \lambda^2 \frac{\sigma_x b D_{av}^2}{4n}.$$

Thus, for a central piece of small size $\lambda < 1$, the bending moment is also directly proportional to a square of a parameter λ.

The most important conclusion from the analysis of schemes discussed above is a possibility of reducing bending schemes with any number of points to a three-point scheme, the analysis of which is the main focus further on.

Three-point scheme of a piece destruction along *xy*-plane. Fig. 3 indicates a generalized three-point calculation scheme for a piece destruction along *xy*-plane (*y*-axis is perpendicular to the figure plane) in an inhomogeneous force field for the maximum possible horizontal displacement of contact forces by a characteristic value ($z_x/2$). This value is equal to half the width of a central zone of a discrete load, which, in accordance with the above considerations, is determined from the expression

$$z_x = \begin{cases} c, & \lambda < 1 \\ D_{av}, & \lambda \geq 1 \end{cases}. \tag{5}$$

The location of a destruction plane is close to a real one, since it passes through point *A* with the highest tensile stresses for the piece upper plane, and also near the point of contact C_3, where the maximum tensile stresses occur for the piece's lower plane. This leads to a formation of surface cracks with their subsequent development into the main crack, dividing the piece into two parts.

In this case, we will ignore contact stresses in favor of nonlocal strength criteria [12], in particular, using the fact that dangerous tensile stresses from bending in a piece of rock (point *A*), determined using the beam scheme, practically coincide with the ultimate strength for uniaxial tension of the piece.

From a standpoint of continuum mechanics, normal stresses are applied to the horizontal and vertical faces of a piece σ_x and σ_z, as well as the tangent stresses τ, the angle of deviation of the maximum main stress from *x*-axis is α.

From the condition of equality of the discrete and equivalent continuous loads on the area z_x, the relations are obtained

$$P_x = \frac{\sigma_x b z_x}{n \cos\alpha_x} = \frac{\tau b z_x}{n \sin\alpha_x}; \tag{6}$$

$$\alpha_x = \arctan\left(\frac{\tau}{\sigma_x}\right). \tag{7}$$

Characteristic values in a piece loading diagrams (Fig. 3) are as follows:

- transverse force

$$Q_1 = \frac{P_x}{2n}\cos\alpha_x - \frac{\tau ab}{n}; \quad Q_2 = \frac{P_x}{2n}\cos\alpha_x + \frac{\tau ab}{n};$$

- bending moment

$$M_1 = \frac{P_x a}{4n}\sin\alpha_x - \frac{\tau ab z_x}{4n};$$
$$M_2 = \frac{P_x a}{4n}\sin\alpha_x + \frac{P_x z_x}{4n}\cos\alpha_x - \frac{\tau ab z_x}{2n};$$
$$M_3 = \frac{P_x a}{4n}\sin\alpha_x + \frac{P_x z_x}{4n}\cos\alpha_x;$$

- longitudinal force

$$N_1 = \frac{\sigma_z ab}{n} - \frac{P_x}{2n}\sin\alpha_x; \quad N_2 = \frac{\sigma_z ab}{n} + \frac{P_x}{2n}\sin\alpha_x.$$

The most dangerous point in the cross-section along *xy*-plane is point *A*.

Stresses along *z*-axis near point *A* from the action of bending in combination with longitudinal compression:

- from the left

$$\sigma_{zA,L} = \frac{N_1}{F_{xy}} - \frac{M_2}{W_{y,xy}};$$

- from the right

$$\sigma_{zA,R} = \frac{N_2}{F_{xy}} - \frac{M_3}{W_{y,xy}},$$

where $W_{y,xy}$ is section modulus of a piece relatively to *y*-axis in *xy*-plane, which, considering the facts described in [11], for a given shape of pieces is determined as follows

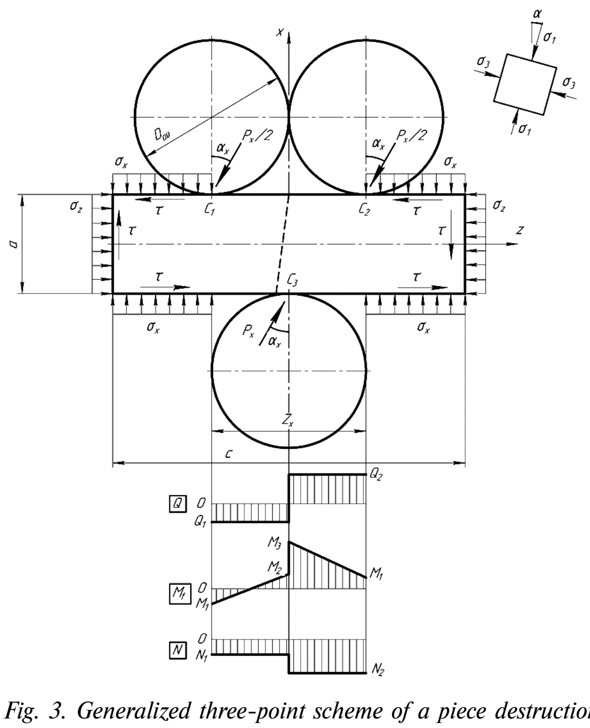

Fig. 3. Generalized three-point scheme of a piece destruction along xy-plane

$$W_{y,xy} = k_f \frac{\pi a^2 b}{32};$$

F_{xy} is a cross-sectional area of a piece

$$F_{xy} = k_f^{2/3} \frac{\pi ab}{4}.$$

Here, as in expression (2), tensile stresses have a “minus” sign, and compressive stresses have a “plus” sign to simplify the notation, since all equivalent destructive stresses are reduced to compressive strength of a rock.

For point A, the following relations are true

$$\sigma_{xA} = 0; \quad \tau_A = 0,$$

therefore, the main stresses at point A have the form

$$\sigma_{1A} = \sigma_{zA}; \quad \sigma_{3A} = 0.$$

Equivalent destructive stress at point A for this calculation case is determined considering (2)

$$\sigma_{eA} = \max(\sigma_{eA,L}; \sigma_{eA,R}).$$

Two-point scheme of a piece destruction along *xy*-plane. A destruction scheme, considered in Fig. 3, is only one of the possible variants of a force scheme, with the maximum relative horizontal displacement of contact forces by the value ($z_x/2$). In this case, bending moment from vertical components of contact forces also reaches the maximum, which is important for pieces with a large relative length k_{ca}.

When decreasing a parameter k_{ca}, the influence of bending is reduced in favor of a shear along the path between the contact points on a piece surface. The shortest trajectory of shear is at zero horizontal displacement of contact forces, which is shown in Fig. 4. This corresponds to a two-point scheme of a piece destruction along *xy*-plane.

Relations (5, 6, and 7) are also true here.

Characteristic values in a piece loading diagrams (Fig. 4) are as follows:

- transverse force

$$Q_4 = \frac{\tau ab}{n};$$

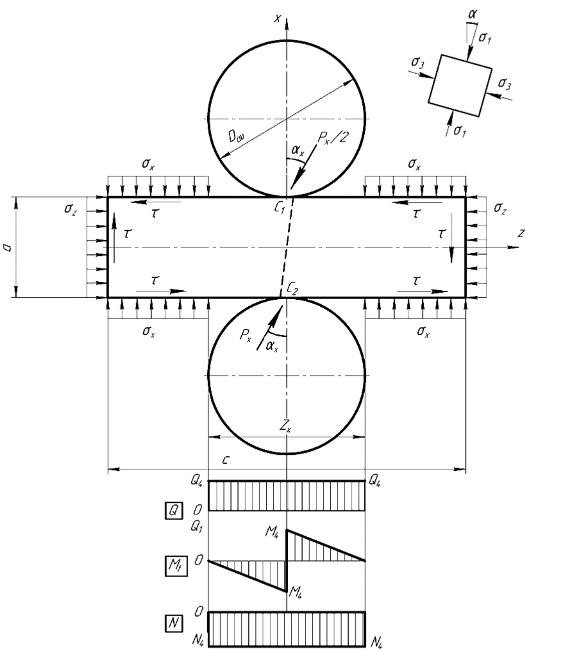

Fig. 4. Generalized two-point scheme of a piece destruction along xy-plane

- bending moment

$$M_4 = \frac{P_x a}{2n} \sin\alpha_x = \frac{\tau abz_x}{2n};$$

- longitudinal force

$$N_4 = \frac{\sigma_z ab}{n}.$$

The highest tensile stresses on the piece upper plane are observed near (to the right) of point C_1, and on the lower plane – near (to the left) of point C_2. Therefore, the main crack practically coincides with the cross-section C_1C_2, which is considered to be the most dangerous.

The maximum horizontal normal stresses in the vicinity of points C_1 and C_2 are determined by the formula

$$\sigma_{zC} = \frac{\sigma_z}{n} - \frac{M_4}{W_{y,xy}}.$$

The equivalent destructive stress for a case of a piece shear is determined from the expression [8]

$$\sigma_{eC} = \frac{(\psi - 1)\sigma_{zC} + \sqrt{(1-\psi)^2 \sigma_{zC}^2 + 4\psi\tau_C^2}}{\psi},$$

where average shear stress is determined by the formula

$$\tau_C = \frac{P_x \cos\alpha_x}{nF_{xy}} - \frac{\tau}{n}.$$

Three-point scheme of a piece destruction along *yz*-plane. The scheme in Fig. 3 is relevant in a case when the direction of the maximum main stress in a layer σ_1 deviates from the x-axis by an angle less than or slightly greater than 45 degrees. In a case when the direction of σ_1 is close to z-axis, a possibility of destroying a piece along the cross-section in the *yz*-plane should also be considered, especially for a piece shape close to the isometric one and at high values of the side thrust coefficient ξ.

The force scheme of piece destruction along a cross-section in *yz*-plane is shown in Fig. 5. Here, the contact points are displaced relatively to each other vertically by the maximum possible value ($x_z/2$), which is determined according to the expression

$$x_z = \begin{cases} a, & \lambda < k_{ca} \\ D_{av}, & \lambda \geq k_{ca} \end{cases}.$$

From a condition of equality of a discrete and an equivalent continuous load at the area z_x, the following relations are obtained

$$P_z = \frac{\sigma_z b x_z}{n\cos\alpha_z} = \frac{\tau b x_z}{n\sin\alpha_z}; \quad \alpha_z = \arctan\left(\frac{\tau}{\sigma_z}\right).$$

Characteristic values in a piece loading diagrams (Fig. 5) are as follows:

- transverse force

$$Q_5 = \frac{P_z}{2n}\cos\alpha_z + \frac{\tau bc}{n}; \quad Q_6 = \frac{P_z}{2n}\cos\alpha_z - \frac{\tau bc}{n};$$

- bending moment

$$M_5 = \frac{P_z c}{4n}\sin\alpha_z - \frac{\tau bcx_z}{4n};$$

$$M_6 = \frac{P_z c}{4n}\sin\alpha_z + \frac{P_z x_z}{4n}\cos\alpha_z;$$

$$M_7 = \frac{P_z c}{4n}\sin\alpha_z + \frac{P_x z_x}{4n}\cos\alpha_z - \frac{\tau bcx_z}{2n};$$

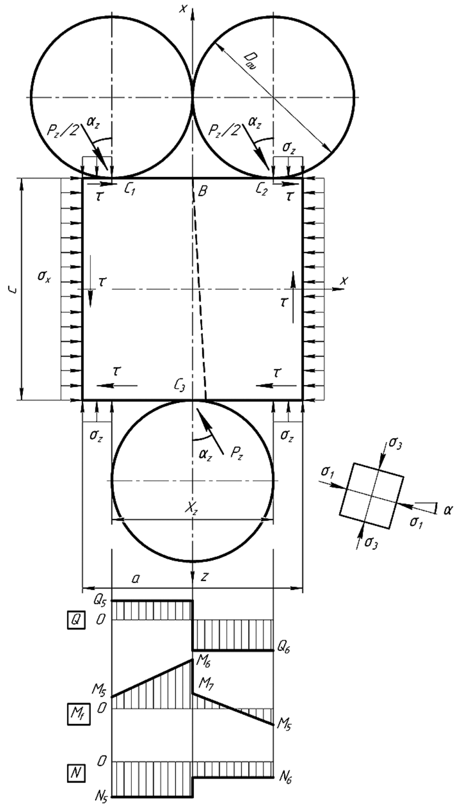

Fig. 5. Generalized three-point scheme of a piece destruction along yz-plane

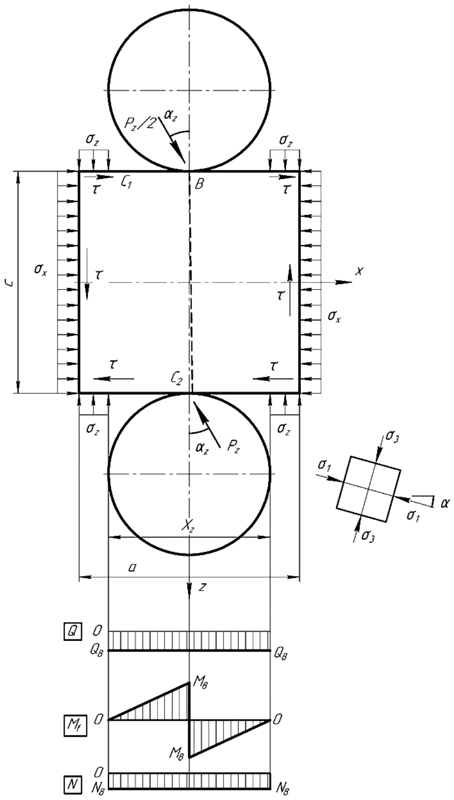

Fig. 6. Generalized two-point scheme of a piece destruction along yz-plane

- longitudinal force

$$N_5 = \frac{\sigma_x bc}{n} + \frac{P_z}{2n}\sin\alpha_z; \quad N_6 = \frac{\sigma_x bc}{n} - \frac{P_z}{2n}\sin\alpha_z.$$

The most dangerous point in a cross-section along *yz*-plane is point *B*.

Stresses along *x*-axis near point *B* from the action of bending in combination with longitudinal compression are:

- from the left

$$\sigma_{zB,L} = \frac{N_5}{F_{yz}} - \frac{M_6}{W_{y,yz}};$$

- from the right

$$\sigma_{zB,R} = \frac{N_6}{F_{yz}} - \frac{M_7}{W_{y,yz}},$$

where $W_{y,yz}$ is section modulus of a piece relatively to *y*-axis in *yz*-plane, which is defined as follows

$$W_{y,yz} = k_f \frac{\pi c^2 b}{32}.$$

F_{yz} is cross-sectional area of a piece

$$F_{yz} = k_f^{2/3} \frac{\pi cb}{4}.$$

For point *B*, the following relations are true

$$\sigma_{zB} = 0; \quad \tau_B = 0,$$

therefore, the main stresses at point *B* have the form

$$\sigma_{1B} = \sigma_{xB}; \quad \sigma_{3B} = 0.$$

The equivalent destructive stress at point *B* for this calculation case is determined considering (2)

$$\sigma_{eB} = \max(\sigma_{eB,L}; \sigma_{eB,R}).$$

Two-point scheme of a piece destruction along *yz*-plane.

Similar to the case of destruction by a shear across the long side of a piece (Fig. 4), Fig. 6 indicates a scheme of destruction by a shear along the shortest path between contact points located on the short sides of a piece.

Characteristic values in a piece loading diagrams (Fig. 6) are as follows

- transverse force

$$Q_8 = \frac{\tau bc}{n};$$

- bending moment

$$M_8 = \frac{P_z c}{2n}\sin\alpha_z = \frac{\tau bc x_z}{2n};$$

- longitudinal force

$$N_8 = \frac{\sigma_z bc}{n}.$$

The maximum horizontal normal stresses in the vicinity of points C_1 and C_2 are determined by the formula

$$\sigma_{xC} = \frac{\sigma_x}{n} - \frac{M_8}{W_{y,yz}}.$$

The equivalent destructive stress for a case of a piece shear is determined from the expression [8]

$$\sigma_{eC,2} = \frac{(\psi-1)\sigma_{xC} + \sqrt{(1-\psi)^2\sigma_{xC}^2 + 4\psi\tau_{C,2}^2}}{\psi},$$

where average shear stress is determined by the formula

$$\tau_{C,2} = \frac{P_z\cos\alpha_z}{nF_{yz}} - \frac{\tau}{n}.$$

Main research results. The force schemes of piece destruction given above have a random and competing character of implementation. Therefore, the maximum equivalent destructive stress and a condition for piece destruction for the predetermined parameters such as the side thrust coefficient ξ, the angle of piece orientation α, the relative piece size k_{ca} and the relative piece size in layer λ is determined by the formula

$$\sigma_e = \max(\sigma_{eA}, \sigma_{eC}, \sigma_{eB}, \sigma_{eC,2}) \geq R_c. \quad (8)$$

Fig. 7 indicates relative dependences for the main components of formula (8), depending on the angle of piece orientation in space when $\xi = 0.22$ and values $k_{ca} = 1.5$ (*a*) and $k_{ca} = 2.0$ (*b*) for pieces of small size ($\lambda < 1$).

For the case in Fig. 7, *a*, bending destruction across the long side is more likely in a range of approximately 0 to 45 degrees, shear destruction across the long side at angles of 45 to 70 degrees. Also, bending destruction across the short side is more likely at angles of 70 to 90 degrees, and shear destruction across the short side is not realized. At the same time, in a range from 0 to 70 degrees, when destruction occurs along the cross-section in *xy*-plane, fragments with a lower coefficient k_{ca} than in the original piece are obtained, i.e. the shape of fragments improves and gets closer to the isometric shape. In a range from 70 to 90 degrees, on the contrary, the shape of fragments worsens, they become more elongated than the original piece.

For the case in Fig. 7, *b*, there is destruction only from bending across the long side for any values of α, the shape of fragments always improves compared to a shape of the original piece. This conclusion is particularly true for even larger values of k_{ca}.

In practice, rock pieces with k_{ca} values less than 1.5 are very rare, and the share of pieces in a range of k_{ca} up to 2.0 even for cube-shaped crushed stone is about 40–50 %, i.e. slightly less than half. In addition, as follows from the graphs in Fig. 7, *a*, (above), even if a piece shear scheme is implemented, the destructive stresses still approximately correspond to the values for a bending scheme. Therefore, the maximum impact on a destruction of small pieces is exerted by the cases of their loading specifically by bending loads.

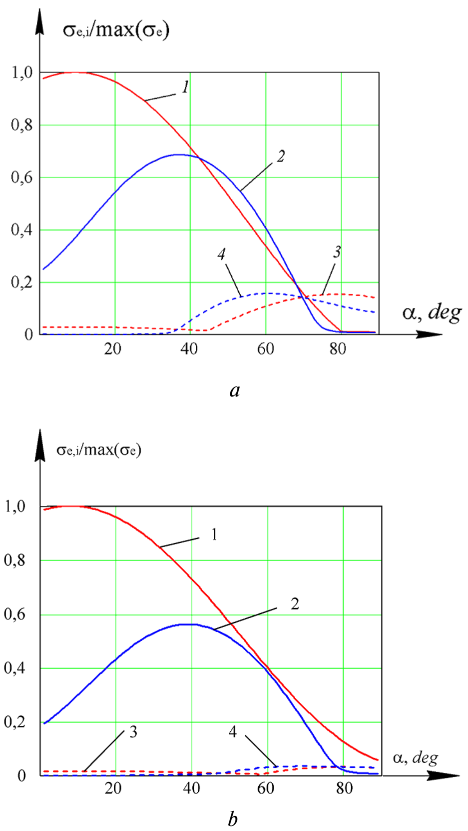

Fig. 7. Equivalent destructive stresses for various force schemes depending on the angle of piece orientation at $\lambda < 1$ and $\xi = 0.22$:

1 – σ_{eA}; 2 – σ_{eC}; 3 – σ_{eB}; 4 – $\sigma_{eC,2}$

Fig. 8 indicates relative dependences for the main components of formula (8) depending on the angle of piece orientation in space when $\xi = 0.22$ and $k_{ca} = 2.0$ for large pieces ($\lambda = 3 > k_{ca}$).

Here, the destruction occurs in the shear force schemes, not the bending schemes, at almost any values of α. Also, it is true in a range from 0 to approximately 70 degrees along the cross-section in *xy*-plane, with a decrease in k_{ca} for fragments, and in a range from 70 to 90 degrees along the cross-section in *yz*-plane, with a deterioration in shape of fragments.

The graphs of destructive stresses with an increase in the side thrust coefficient, for example, up to $\xi = 0.5$ are of particular interest, what occurs when the rock mass layer is compacted in a process of its deformation, both for small pieces ($\lambda < 1$, Fig. 9, *a*), and for large pieces ($\lambda = 3$, Fig. 9, *b*). Here $k_{ca} = 2.0$.

As seen from the analysis of graphs, small pieces are destroyed exclusively by bending across the long side, and the large ones are destroyed by shear across the long side over the entire range of angles α, with a decrease in the parameter k_{ca} for fragments, i.e., increasing the uniformity of a force field improves the shape of pieces, bringing it closer to the isometric shape.

Conclusions. An analytical model of destruction of pieces with random shape in disintegrators under loading in a thick layer of rock mass has been created. The considered piece has a rectangular shape, while the particles around it are modeled in a round shape.

Formulas for equivalent destructive stresses in a piece are obtained for variants of bending and shear force schemes, when discrete contact forces are applied to the long or the short sides of a piece.

Dependences in relative values of equivalent destructive stresses on an angle of piece orientation relative to direction of the maximum main stress in a rock layer are obtained.

It was established that the destruction of pieces occurs as a result of implementation of predominantly bending destruction schemes, which is especially important at high values of relative piece length k_{ca}, small relative piece size in a layer λ and application of the main load across the long side. In this case, the shape of piece fragments usually improves, their relative length k_{ca} is smaller compared to the original piece.

Increasing a uniformity of a force field with an increase in side thrust coefficient ξ also improves the shape of piece fragments.

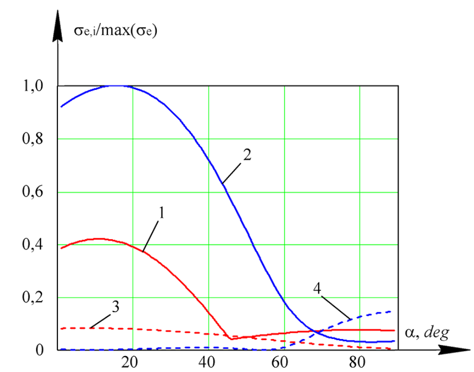

Fig. 8. Equivalent destructive stresses for various force schemes depending on the angle of piece orientation at $\lambda = 3$ and $\xi = 0.22$:

1 – σ_{eA}; 2 – σ_{eC}; 3 – σ_{eB}; 4 – $\sigma_{eC,2}$

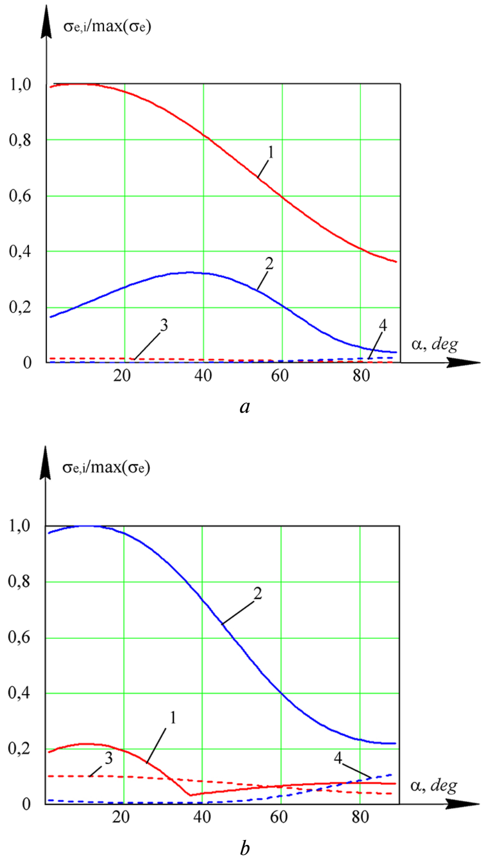

Fig. 9. Equivalent destructive stresses for various force schemes depending on the angle of piece orientation at $\xi = 0.5$*:*
1 – σ_{eA}*; 2 –* σ_{eC}*; 3 –* σ_{eB}*; 4 –* $\sigma_{eC,2}$

In the case of a piece shape close to the isometric one $k_{ca} \to 1$, a high relative piece size in a layer λ and application of the main load across the short side, the probability of implementing shear schemes increases compared to bending schemes, a significant share of fragments worsens their shape compared to the original piece.

Thus, it has been analytically proven, that disintegration in a thick layer leads to a lower level of destructive stresses for destruction of small lamellar pieces compared to large isometric ones, which explains the effects of improving the shape of pieces and accelerated destruction of smaller fractions.

References.

1. Bozhyk, D. P., Sokur, M. I., Biletskii, V. S., Shevchuk, Yu. V., & Sokur, I. M. (2017). Research or the state and development of production of cotstructiot materials from natural building stone. *Zbahachennia korysnykh kopalyn, naukovo-tekhn. zbirnyk*, *68*(109), 3-12.
2. Sokur, M. I., Biletskii, V. S., Vedmid, I. A., & Robota, Ye. M. (2020). *Ore preparation (crushing, grinding, classification): monograph*. Kremenchutskyi Natsionalnyi Universytet im. M. Ostrohradskoho, Akademiia Hyrnychykh Nauk Ukrainy: PP Shcherbatykh O. V., Kremenchuk.
3. Sokur, M. I., Biletskii, V. S., Yehurnov, O. I., Vorobyov, O. M., Smyrnov, V. O., & Bozhyk, D. P. (2017). *Preparation of minerals for enrichment: monograph*. Kremenchutskyi Natsionalnyi Universytet im. M. Ostrohradskoho, Akademiia Hyrnychykh Nauk Ukrainy: PP Shcherbatykh O. V., Kremenchuk.
4. Nadutyi, V., Tytov, O., & Cheberiachko, I. (2018). Hereditary model of loose mined rock layer deformation in disintegrators. *E3S Web of Conferences, Ukrainian School of Mining Engineering*, *60*, 00033. https://doi.org/10.1051/e3sconf/20186000033.
5. Solona, O. V. (2020). Controlled vibrating mill for grinding bulk medium. *Vibratsii v tekhnitsi ta tekhnolohiiakh*, *4*(99), 11-20.
6. Belmas, I., Kogut, P., Kolosov, D., Samusia, V., & Onyshchenko, S. (2019). Rigidity of elastic shell of rubber-cable belt during displacement of cables relatively to drum. *International Conference Essays of Mining Science and Practice*, *109*, 00005. https://doi.org/10.1051/e3sconf/201910900005.
7. Ilin, S., Adorska, L., Samusia, V., Kolosov, D., & Ilina, I. (2019). Conceptual bases of intensification of mining operations in mines of Ukraine based on monitoring and condition management of mine hoisting systems. *International Conference Essays of Mining Science and Practice*, *109*, 00030. https://doi.org/10.1051/e3sconf/201910900030.
8. Babets, D., Sdvyzhkova, O., Shashenko, O., Kravchenko, K., & Cabana, E. C. (2019). Implementation of probabilistic approach to rock mass strength estimation while excavating through fault zones, *Mining of Mineral Deposits*, *13*(4), 72-83. https://doi.org/10.33271/mining13.04.072.
9. Sdvyzhkova, O., Golovko, Y., Dubytska, M., & Klymenko, D. (2016). Studying a crack initiation in terms of elastic oscillations in stress strain rock mass, *Mining of Mineral Deposits*, *10*(2), 72-77.
10. Pryadko, N. C., & Ternovaya, E. V. (2016). Controlled vibrating mill for grinding bulk medium. *Tekhnicheskaya Mekhanika*, (4), 104-111.
11. Nadutyi, V. P., Tytov, O. O., Kolosov, D. L., & Sukhariev, V. V. (2020). Influence of particles geometry on the efficiency of operation of quasistatic and inertial disintegrators, *Naukovyi Visnyk Natsionalnoho Hirnychoho Iniversytetu*, (6), 21-27. https://doi.org/10.33271/nvngu/2020-6/021.
12. Efimov, V. P. (2016). Determination of tensile strength of rocks based on the results of testing disk samples with a central hole. *Fiziko-tekhnicheskie problemy razrabotki poleznykh iskopaemykh*, *5*, 54-60.

Плоска задача визначення зусиль для руйнування шматків у дезінтеграторах при захопленні товстим шаром

О. О. Титов[1], *В. П. Надутий*[2], *К. В. Бабій*[2], *Д. Л. Колосов*[1], *В. Ю. Кухар*[1]

1 – Національний технічний університет "Дніпровська політехніка", м. Дніпро, Україна, e-mail: tytov.o.o@nmu.one
2 – Інститут геотехнічної механіки імені М. С. Полякова, м. Дніпро, Україна

Мета. Встановлення аналітичних залежностей руйнівних напружень, що діють на шматок неізометричної форми під час квазістатичної деформації відносно товстого шару гірничої маси в дезінтеграторах, від параметрів форми шматка, просторової орієнтації шматка, а також відносної крупності шматка у шарі, з урахуванням дискретного характеру прикладання контактних зусиль.

Методика. Плоска схема контактів шматка неізометричної форми в товстому шарі гірничої маси отримана через композицію центрального прямокутного шматка та круглих шматків середнього для даного шару розміру. Розподіл компонентів напружень у шарі гірничої маси прийнято на основі класичної теорії пружності й теорії сипкого середовища. В якості критерію руйнування шматка у складному напруженому стані використано критерій геомеханіки, що показує зв'язок еквівалентного руйнівного напруження й межи міцності породи на стиск. Усі силові схеми навантаження шматка зведені до триточкових схем вигину й двоточкових схем зрізу, як поперек довгої, так і поперек короткої сторін шматка, з аналізу яких находимо найбільш небезпечний у конкретному випадку варіант. Застосована безрозмірна параметризація як для завдання геометричних параметрів шматків, так і для аналізу сумарних руйнівних напружень.

Результати. Отримані аналітичні залежності еквівалентних руйнівних напружень для шматка витягнутої форми в залежності від відносної довжини шматка, відносної крупності шматка у шарі, кута орієнтації шматка відносно напряму максимального головного напруження й коефіцієнта бічного розпору у шарі породи. Установлено, що лещадні шматки, особливо ті, що є дрібні-

шими за середній розмір у шарі, руйнуються переважно від реалізації схем вигину поперек довгої сторони, форма уламків поліпшується за рахунок зменшення відносної довжини шматка. Підвищення однорідності силового поля в робочій зоні дезінтегратора також призводить до поліпшення форми уламків. З іншого боку, у міру наближення форми шматка до ізометричної, а також збільшення відносної крупності шматка у шарі, зростає ймовірність реалізації схем зрізу та зменшується ймовірність реалізації схем вигину, у тому числі з погіршенням форми уламків порівняно з вихідним шматком. При цьому доведена аналітично наявність більших величин руйнівних напружень для лещадних дрібних шматків порівняно з ізометричними великими, за інших рівних умов.

Наукова новизна. Обґрунтована універсальність застосування триточкової схеми вигину шматка неізометричної форми в поєднанні зі двоточковою схемою його зрізу для аналізу руйнування в товстому шарі гірничої маси. Уперше отримані залежності еквівалентних руйнівних напружень для неізометричного шматка від його відносної довжини, його відносної крупності у шарі, кута відхилення головної осі шматка від напрямку головного напруження й коефіцієнта бічного розпору у шарі.

Практична значимість. Отримані результати дозволять здійснювати обґрунтований вибір параметрів робочих органів дезінтеграторів для руйнування матеріалів у товстому шарі, а також прогнозувати зміну частки лещадних шматків у процесі дезінтеграції. Вони дають змогу визначити ключові параметри робочих органів для нових конструкцій дезінтеграторів. Це створює основу для розробки методик розрахунку робочих органів сучасних зразків дробарно-подрібнювального обладнання.

Ключові слова: *дезінтегратор, товстий шар, складний напружений стан, лещадний шматок, вигин, зріз, коефіцієнт бічного розпору*

The manuscript was submitted 27.04.21.